Spatiotemporal relationships, influencing factors and policy implications of coastal man–land system spatial resilience based on interpretable machine learning models: A case study of China's southeastern coastal region

Huan Song[1¶], Zeyu Wang[2*]

[1] School of Geography, Liaoning Normal University, Dalian, Liaoning, China

[2] Institute of Marine Sustainable Development, Liaoning Normal University, Dalian, Liaoning, China

[*]Corresponding author
E-mall: wangzeyu2008@163.com

Abstract

Spatial resilience, as a projection of system resilience at the landscape scale, offers a novel spatial interpretation for analyzing man–land interactions in coastal zones. This study builds an evaluation system from "element-landscape-system" levels, based on the conceptual framework of spatial resilience in coastal man–land systems. It examines the spatiotemporal evolutionary features of spatial resilience at various scales using multisource spatiotemporal big data. Interpretable machine learning techniques were used to construct SHapley Additive exPlanations (SHAP) models and investigate influencing factors. Results yielded three main findings: First, spatial resilience of man–land systems in the southeastern coastal region exhibits significant spatiotemporal heterogeneity with a slow optimization trend, forming a multi-scale spatial pattern characterized by "higher resilience in the element layer in the north than in the south, higher resilience in the landscape layer along the coast than in bays, and stronger resilience in the system layer in the north than in the south." Second, habitat quality, landscape connectivity index, and marine aquaculture area were the core factors influencing spatial resilience at the element, landscape, and system levels, contributing 35.17%, 29.24%, and 28.87%, respectively. Third, the variables with higher contribution rankings exhibited threshold effects on spatial resilience at different scales. To promote integrated land–sea management and optimize territorial spatial layout, this study, based on the advantages of regional resource endowments, formulates differentiated zonal management strategies and puts forward targeted policy recommendations.

Keywords

Coastal man–land system; Spatial resilience; Interpretable machine learning; Threshold; Southeastern coastal region

Introduction

The 2030 Agenda for Sustainable Development (Sustainable Development Goals, SDGs), released by the United Nations in 2015, has further directed man–land system research toward Earth's surface environmental change, sustainable development goals, coupling processes, and spatial patterns between humans and land [1, 2]. As a critical zone for man–land interaction, China's coastal regions account for only 13% of the territory but contain over 70% of large and medium-sized cities, 45% of the population, and nearly 60% of the GDP. Long-term land reclamation has fragmented habitats, port development has reduced landscape connectivity, and enclosed aquaculture has disrupted ecological substrate continuity. These processes weaken marine ecological functions and services and compress the self-regulation space of coastal man–land systems, thereby reducing their disturbance resilience and pushing them toward critical recovery thresholds [3, 4]. Thus, addressing the SDGs by mitigating conflicts between coastal socioeconomic development and resource-carrying capacity, and restoring the resilience of man–land systems, has become a major research focus. Spatial resilience, which considers the spatial attributes of system variables and interprets resilience from a landscape perspective, clarifies man–land dynamics, post-disturbance recovery paths, and multi-scale spatial correlations. This aligns with the current need to manage coastal ecological disturbances and promote sustainable man–land development [5]. Thus, analyzing man–land coupling through spatial resilience enriches the "pattern–process–service–sustainability" paradigm in landscape ecology and improves the effectiveness of coastal ecological restoration.

In 1973, Holling introduced the concept of resilience into ecological research, defining it as a system's capacity to absorb changes in state variables, driving variables, and parameters while maintaining its stability [6]. In parallel, the social-ecological systems (SES) framework was introduced with the core aim of strengthening the coupling between ecological and social systems [7]. These two strands of research gradually converged and developed. Building on Holling's adaptive cycle theory [8], SES research has begun to focus on systems' adaptive capacity and their dynamic responses to external disturbances [9, 10]. As resilience spread across disciplines, its meaning and methods became more diverse and sophisticated. Since the 2000s, after Adger et al. (2000) extended resilience to the social sciences, studies have increasingly addressed social systems, communities, groups, and individuals [11]. This broadened scope reflects a shift from viewing resilience mainly as the capacity to recover from disturbances to emphasize adaptation, transformation, and learning in socio-ecological systems [12, 13]. For evaluation and quantification, Cutter's DROP model and the BRIC index measured community resilience to disasters across multiple dimensions [14, 15]. Chinese scholars have also developed localized indicator systems for arid regions, tourist areas, and mountain villages [16–19]. Regarding influencing factors, a multidimensional perspective has emerged, spanning ecological elements such as landscape connectivity and biodiversity [20, 21].; economic and technological attributes, such as industrial structure and resource use efficiency [22, 23].; and institutional and social dimensions, including policy regulation and governance mechanisms [24, 25]. On this basis, Fu et al. (2020) proposed using spatial thresholds

to understand system states and man–land dynamics, promoting a shift from studies of single ecosystems or regions to a “multi-factor, multi-process, multi-scale” approach [26]. At the elemental scale, Salvati et al. (2013) used climate, soil, and vegetation to identify environmentally sensitive areas, strengthening the micro-foundation of spatial resilience [27]. At the landscape scale, Luo et al. (2018) showed that the spatial configuration of landscape variables directly affects resilience levels [28]. At the system scale, Chuang et al. (2018) grouped community resilience indicators into local, tele-connected, and socio-ecological dimensions [29]. Furthermore, Hao and Fu (2025) identified landscape connectivity as a key link between natural and socio-economic factors in the formation of spatial resilience [30, 31].

From a landscape ecology perspective, Cumming (2011) defined spatial resilience as the combined effect of internal and external variables acting on a system across multiple spatiotemporal scales [32]. Its key distinction from traditional resilience assessment is its focus on the dynamics of spatial patterns and neighborhood interactions. Rather than concentrating only on vulnerability or risk, spatial resilience in coastal man–land systems emphasize the adaptive governance between human activities and marine/nearshore terrestrial ecosystems, including both exploitation and conservation, as well as ecological feedback and constraints on human use [33, 34]. However, existing work has three main gaps. First, research practices exhibit “land–centric bias” and land–sea fragmentation limitations, overlooking the holistic and interactive nature of their convergence zones. Existing outcomes, grounded in “man–land systems,” overly focus on isolated terrestrial areas or coastal wetlands. Failing to

leverage the integrated land–sea advantages of man–land systems, hindering the depiction of the three-dimensional coupling between humans, oceans, and nearshore terrestrial areas. Second, inadequate integration across research scales, lacking coordinated land–sea design at the "element-landscape-system" levels, hinder the representation of spatial resilience's logic: "micro-level support, meso-level regulation, and macro-level feedback." Third, methodological limitations, research relies mainly on linear tools, such as index decomposition and panel regression, which cannot adequately capture nonlinear, dynamic relationships. Studies that employ machine learning often lack interpretability, leaving the mechanisms of influence unclear. Interpretable machine learning has garnered significant attention because of its ability to capture complex nonlinear patterns without stringent model assumptions. Combined with interpretability tools such as SHapley Additive exPlannation (SHAP), it allows the quantification of contribution and threshold effects of driving factors, providing a new approach to uncover the mechanisms that shape spatial resilience.

China's southeastern coastal region, a key frontier for opening to the world and a major economic growth engine, is one of the world's richest areas in coastal wetlands. It features high population density, intensive economic activity, and heavy pressure on resources and environmental carrying capacities. Rapid industrialization and urbanization, together with land reclamation, port construction, and offshore aquaculture, have intensified conflicts between marine ecosystems and human activities. Consequently, wetland degradation, habitat fragmentation, seawater pollution, and weakened coastal ecological functions have become more pronounced, seriously

constraining sustainable socio-economic development in the region [35]. Against this backdrop, this study focused on the southeastern coastal region. First, this study analyzes the spatial resilience of coastal man–land systems at multiple scales. Second, it integrates multisource remote sensing data to build a spatial resilience evaluation framework from an "element-landscape-system" perspective and applies Getis-Ord Gi^* hotspot analysis to identify spatiotemporal evolution patterns. Finally, a machine learning model was developed and combined with SHAP to reveal the nonlinear effects and interactions of multi-scale drivers on spatial resilience. These results provide a solid scientific basis for the ecological zoning of coastal areas.

Materials and methods

Study area

The southeastern coastal region (20°31′–28°14′ N, 108°36′–122°18′ E) is an open coastal zone bordering the East China Sea and South China Sea, with a coastline of over 13,000 km and maritime area of approximately 476,000 km^2. This economically dynamic region, centered on the coastal economic belt, mainly covers Fujian, Guangdong, Hainan, Zhejiang, Shanghai, and other coastal provinces, including 36 coastal cities and 135 coastal counties/districts (Fig 1). Since China's reform and opening-up, this region has used its geographical advantages to become a leading area of economic growth with a strong marine economy. In 2024, the GDP of its coastal cities totaled 32.6 trillion yuan, or 23.5% of China's GDP. However, rapid urbanization has brought serious challenges. Higher population density and energy consumption

have worsened environmental pollution and threatened coastal sustainability. Pollutant discharge from inland areas has exceeded the carrying capacity of coastal zones, adding to ecological pressure. Large-scale land reclamation, port development, and offshore aquaculture have damaged coastal wetlands and natural shorelines and weakened marine biodiversity. Coastal erosion has caused land loss, damage to coastal structures, and degradation of beach ecosystems. Amid the expansion of construction land and industrial scale, marine space and mineral and biological resources are overexploited, intensifying man–land and human–sea conflicts. Therefore, scientific evaluation of spatial resilience in this region is vital for sustainable development. Based on the spatial scale and hierarchical nature of man–land system restoration, this study analyzed 135 coastal counties and districts, 36 coastal cities, and 7 coastal provinces and municipalities in the southeastern coastal region at the micro-, meso-, and macro-levels. The spatial boundary of this study is defined as the coastal zone and its adjacent offshore waters (offshore distance ≤ 20 km), which is consistent with the core area of China's inshore marine management and represents the region with the most intense human–sea interactions. The open ocean area (offshore distance > 20 km) is not included in this study due to its weak direct impact from human activities and limited

data availability.

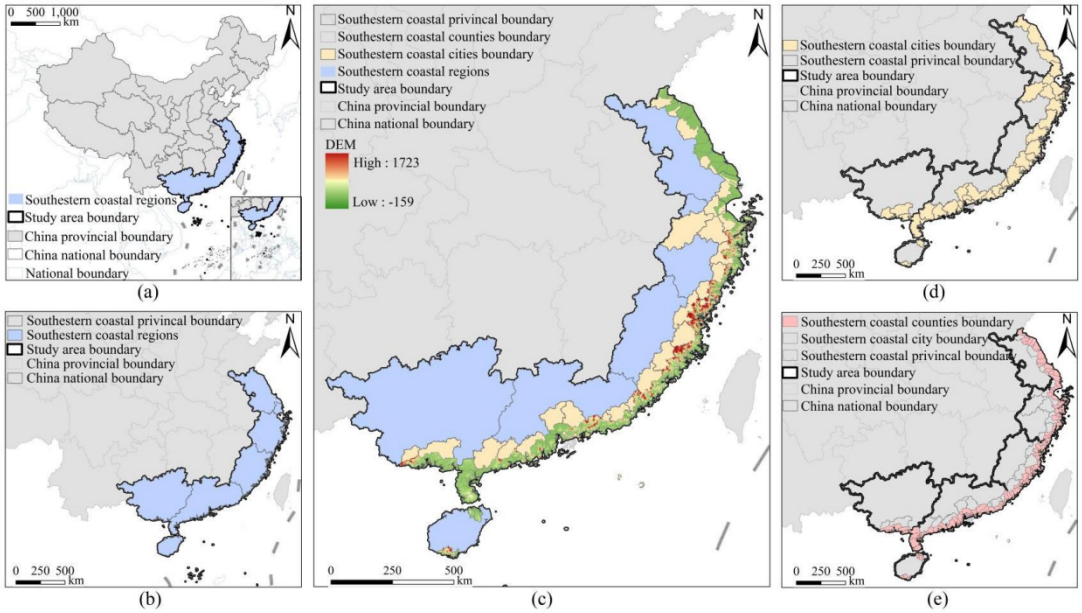

Fig 1. Overview of the study area. (a) Location in China. (b) Scope and division by provinces. (c) Elevation. (d) Division by cities. (e) Division by counties.

Data sources and preprocessing

The required data encompass multiple types and spatiotemporal resolutions, including land-use, socioeconomic, and auxiliary geographic information. The time series covers four years—1990, 2000, 2010, and 2020—to ensure full alignment with the study period. All datasets were unified to the WGS84 coordinate system and resampled to a 1 km resolution. The specific data sources, acquisition, and preprocessing workflows are as follows: (1) Land-use data were obtained from the CLCD land-use dataset (30 m resolution) released by the Institute of Remote Sensing and Digital Earth, Wuhan University (https://irsip.whu.edu.cn/index.php). Using ArcGIS 10.8, the data underwent projection transformation, mosaicking, clipping, and

other preprocessing steps, and were then reclassified into seven categories: forest, grassland, water bodies, wetlands, cropland, built-up land, and unused land. (2) Ecological and geographic data included the Normalized Difference Vegetation Index (NDVI), sourced from the Resource and Environmental Science Data Center of the Institute of Geographic Sciences and Natural Resources Research, Chinese Academy of Sciences (1 km resolution) (www.resdc.cn). Temperature and precipitation data (1 km resolution) were obtained from the National Qinghai-Tibet Plateau Science Data Center (data.tpdc.ac.cn). Vector data for county-, city-, and provincial-level administrative boundaries, as well as DEM data (1 km resolution), were acquired from the Geospatial Data Cloud platform (https://www.gscloud.cn). (3) Socioeconomic data at the provincial/municipal level were derived from the 1990—2020 editions of the China Statistical Yearbook, China Urban Statistical Yearbook, China Marine Economy Statistical Yearbook, China Marine Ecological Environment Bulletin, China Environmental Statistical Yearbook, and the statistical yearbooks/bulletins of provinces and cities in the southeastern coastal region. To spatialize socioeconomic attribute data extracted from these yearbooks, provincial/municipal statistics were integrated with administrative boundary vector data. A spatial join was then applied to generate gridded socioeconomic distribution data with geographic coordinates. ④Indicator standardization and weighting: To eliminate inconsistencies in the dimensions of indicator data, *Z*-score normalization was performed on the raw data using Python, and the normalized values were linearly rescaled to the range [0, 1]. Indicator weights were determined by combining the Analytic Hierarchy Process (AHP) with the entropy

weight method, and composite indicators were subsequently constructed based on these weights [36].

Research process and methodology

Technical approach

The technical approach, illustrated in Fig 2, consists of four main steps: constructing the indicator system, quantifying resilience values, characterizing spatiotemporal patterns, and analyzing influencing mechanisms. a) Indicator system construction: Establish an evaluation indicator system for the spatial resilience of man–land systems and normalize all variables to form a standardized indicator dataset; b) Resilience quantification and pattern detection: Calculate the composite spatial resilience index for each evaluation unit within the man–land system. The Getis-Ord Gi^* statistic was used to identify resilience hotspots and cold spots, and to analyze their spatiotemporal evolution; c) Model selection and regression analysis: Compare the predictive performance of multiple machine learning models and select the optimal model for the regression analysis of spatial resilience; d) Attribution analysis and interpretation: Identify the contribution of each driving factor using the selected machine learning model combined with SHAP-based visualization and explore the underlying nonlinear effects and interaction patterns.

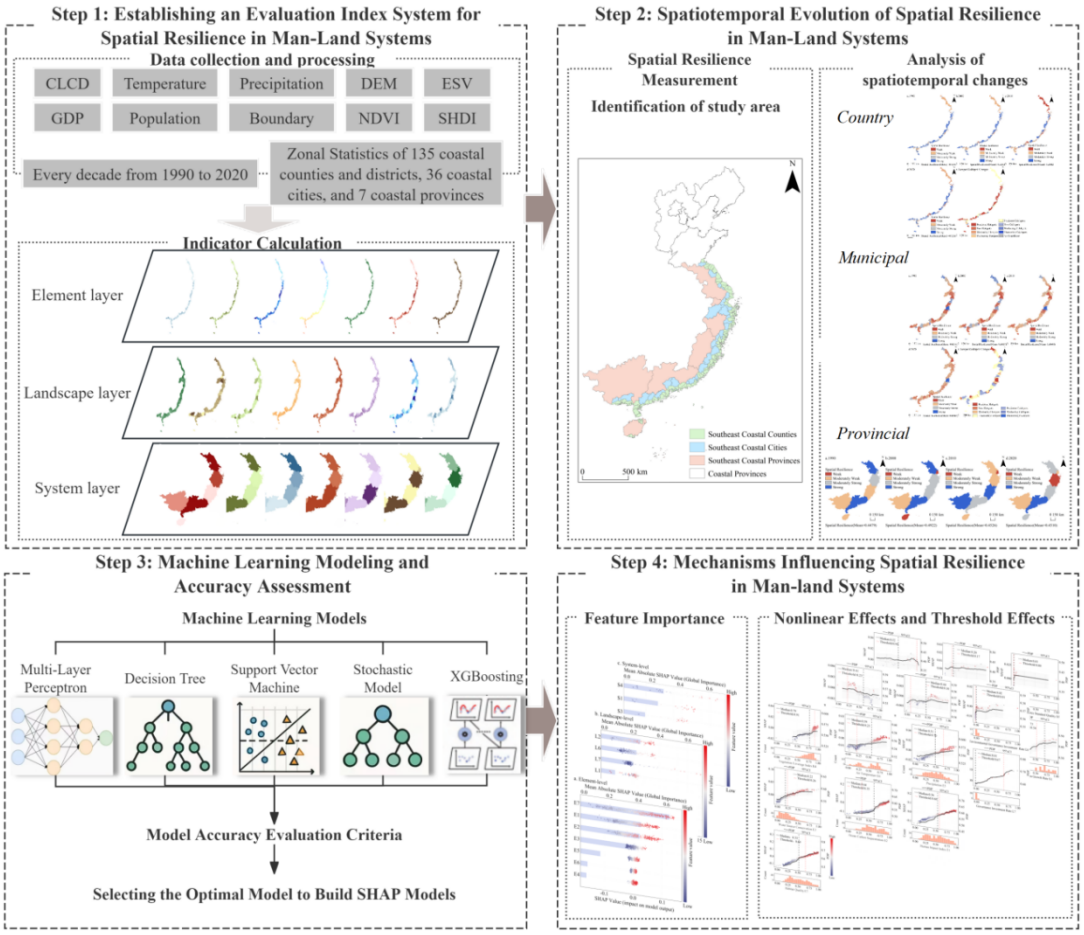

Fig 2. Technical route for the study

Evaluation indicator system

Analysis of spatial resilience in coastal man–land systems

Spatial resilience refers to the capacity of a regional spatial entity to absorb, recover from, or transform under natural and social disturbances while maintaining the structural stability of man–land systems. Compared with traditional resilience studies, it places greater emphasis on the spatial attributes (e.g., location, connectivity, and matrix) of variables within and beyond the system, integrating landscape ecology, resilience theory, and sustainable development concepts [37]. Centered on man–land system dynamics, spatial resilience focuses on the spatial characteristics of landscape

carriers and regulation of human activities. From a multi-scale spatiotemporal dynamic perspective on social-ecological system resilience, resilience is interpreted through the lens of the landscape as a carrier. The coastal man–land system is a complex open mega system formed by the interaction between human activities and the land–sea interface environment of the coastal zone (Li et al., 2018). Its spatial resilience, shaped by distinctive land–sea interaction characteristics, forms a unique theoretical framework that fundamentally differs from that of traditional man–land system resilience, as summarized in Table 1.

Table 1. Conceptual Analysis.

Comparison dimensions	Resilience of traditional man–land systems	Spatial resilience of coastal man–land systems
Core concept	Takes the land-based geographical environment as the core carrier, emphasizing a mainly unidirectional pattern of adaptation and regulation between "humans and terrestrial environments."	Focuses on the land–sea interaction zone as the core domain, emphasizing three-dimensional coupling among "humans, oceans, and nearshore terrestrial areas," with the core being bidirectional adaptation between land–sea ecological processes and human activities.

Key characteristics	Emphasizes maintaining the stability of terrestrial ecosystems.	Highlights three core principles: integrated land–sea management, bidirectional interactions, and ecological service mobility. It breaks administrative and natural boundaries to enable cross-domain regulation of elements, balances the bidirectional feedback between marine ecological services supplied to land and terrestrial human activities impacting the sea, and leverages natural processes to support cross-domain transmission of ecological services between land and sea.
Mechanism of action	Relies primarily on a unidirectional synergy between the self-regulation of terrestrial ecosystems and human intervention.	Builds on the interconnectedness of land–sea ecological processes to establish a closed-loop mechanism of "land disturbance transmission–marine ecological response–land–sea synergistic restoration," requiring consideration of both the continuity of natural processes and the

transboundary nature of human activities.

The "element-landscape-system" multi-scale evaluation framework organically integrates the "pattern–process–scale" theory of landscape ecology with the SES framework [38]. From the perspective of landscape ecology, the element level focuses on the patterns of landscape components, encompassing relatively homogeneous ecological units, such as individual wetland patches, shoreline segments, and vegetation-covered areas. Its core concern is the quality and functioning of ecological components without explicitly addressing the spatial connections among units. The landscape-level focuses on the overall structural pattern of the landscape, including the structure of typical landscape ecological units such as estuaries and bays, comprising patches, corridors, and matrixes, as well as the spatial coordination of economic and ecological functions. Its core lies in the spatial configuration and connectivity of heterogeneous components, emphasizing the optimizing effect of human regulation in shaping the landscape structure. The system-level centers on cross-domain linkage patterns of landscapes, encompassing the holistic coordination of population, resources, and the environment across administrative units. Its core lies in regional-scale collaborative governance and supply–demand balance, highlighting the supportive roles of policy regulation and industrial layout in maintaining overall system stability. These three levels align with the ecological logic of components–structure–function, forming a complete chain in which "patterns shape processes, processes support functions, and functions ensure resilience" [39, 40]. In summary, the spatial resilience

of coastal man–land systems is defined as follows: within the interactive system formed by human activities and the land–sea natural environment in coastal zones, spatial resilience is enhanced through the three-dimensional coupling of people, sea, and space. Considering land–sea coordination as the core principle and spatial structure optimization, functional synergistic adjustment, and multi-scale process linkage as the main pathways, it integrates anthropogenic governance with natural restoration and fully leverages the bidirectional interactions between land and sea and the advantages of ecological service flows. This dynamic process strengthens the system's capacity to recover from and adapt to various natural disturbances (e.g., sea-level rise and extreme weather events) and anthropogenic impacts (e.g., land reclamation, port–adjacent industrial development, and intensive aquaculture) (Fig 3). The specific implementation pathways are as follows. At the element level, through measures such as coastline management and aquaculture–to–beach restoration projects, artificial interventions are combined with ecological design to repair locally damaged structures, translating county-level ecological restoration guidelines into concrete spatial operational pathways. At the landscape-level, focusing on typical landscape ecological units such as estuaries and bays, coastal urban development patterns are adjusted, the spatial configuration of the "patch-corridor-matrix" structure is optimized, and the coordination of economic and ecological functional spaces is promoted, thereby strengthening the linkage between socio-economic development and ecological restoration. At the system level, a spatial balancing mechanism for development and protection was established across administrative units by delineating the marine nature

296 reserve boundaries and coordinating the spatial layout of coastal pollution control.
297 Regional collaborative governance forms a comprehensive spatial restoration
298 framework covering the entire coastal zone.

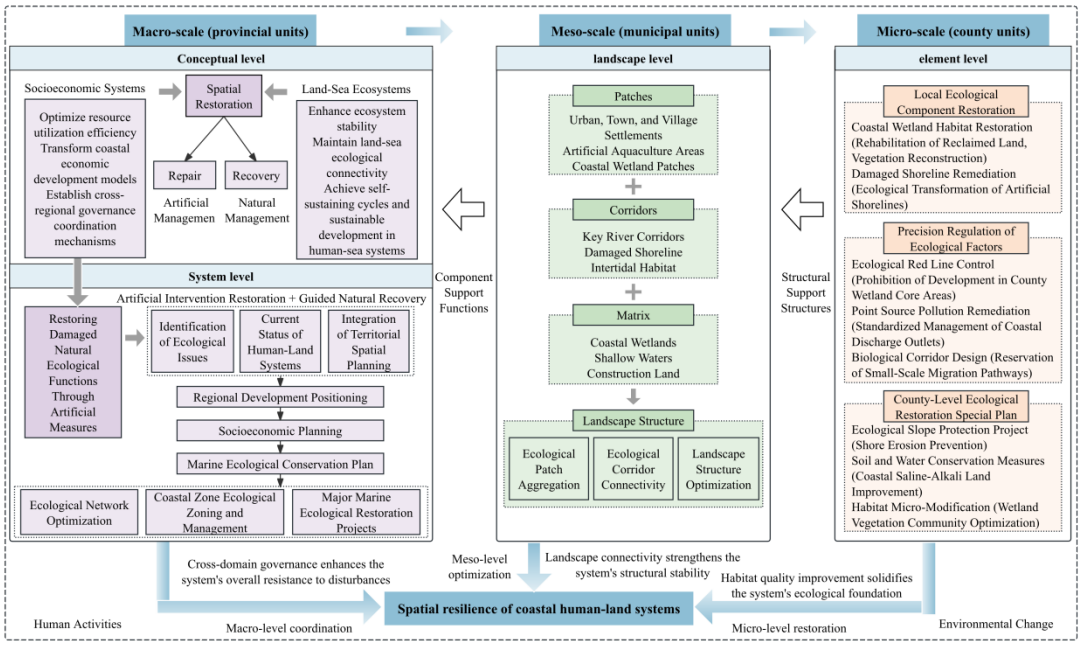

299

300 Fig 3. The framework of spatial resilience in man–land systems

301

302 ## Development of evaluation indicator system

303 Based on the spatial resilience characteristics of coastal man–land systems and the
304 specific conditions of the southeastern coastal region, an evaluation indicator system
305 for spatial resilience is constructed within the “element-landscape-system” framework.
306 This system was designed to analyze the types and potential of man–land system spatial
307 resilience across multiple scales in the southeastern coastal region. County-level
308 administrative units function as decision-making units for spatial restoration at the
309 elemental level. Municipal-level units exhibit relatively independent landscape
310 connectivity characteristics, whereas provincial-level units represent composite

311 systems that integrate socio-economic development and natural ecological conditions.
312 Accordingly, county-, municipal-, and provincial-level administrative units were
313 designated as the evaluation units for the element, landscape, and system layers,
314 respectively. Considering the spatial distribution of man–land system resilience, the
315 evaluation scope is determined according to the following principles: Counties and
316 districts closer to the sea experience greater pressure on coastal ecosystems; therefore,
317 they are prioritized in the evaluation; landscape-level evaluation emphasizes ecological
318 connectivity and thus, covers all element-level units. System-level evaluation must
319 encompass all administrative units within the southeastern coastal region. The
320 evaluation scope included 135 coastal counties/districts, 36 coastal cities, and 7 coastal
321 provinces/municipalities in the southeastern coastal region. The current status and
322 development trends of coastal man–land systems constitute the foundation of spatial
323 restoration. The pressures generated by change processes and the policy and
324 management responses to these pressures are key factors shaping spatial resilience.
325 Following the principles of scientific rigor, effectiveness, representativeness, data
326 availability, and operational feasibility, and drawing on the “Pressure–State–Response”
327 (PSR) framework, we constructed an evaluation indicator system for the spatial
328 resilience of coastal man–land systems based on the “element-landscape-system”
329 approach (Table 2). This system not only builds on existing research on spatial
330 resilience but also refines and supplements indicators specific to coastal human–marine
331 interactions. ①Pressure indicators quantify drivers that directly threaten the stability
332 of coastal human–marine systems, including pressures from human activities and

natural environmental stresses. Element-level: The Human Impact Index characterizes the intensity of human activities associated with different land-use types. Landscape-level: The Landscape Pressure Index, measured using the Shannon Diversity Index [41], reflects the level of stress imposed by human activities on the spatial structure of a landscape. System-level: Population growth rate and the ecological pressure index characterize the macro-level pressures from socio-economic development and pollutant emissions, respectively. Sea-level rise height was used to quantify the threat posed by rising sea levels in the coastal zone. ②State indicators describe the physical, ecological, and economic conditions of the coastal human–marine system under pressure, directly reflecting system health and stability. Element-level: Marine carbon sequestration and water conservation are key ecosystem services. The vegetation coverage index reflects the growth status and extent of the terrestrial vegetation cover. Precipitation and temperature indicate the stability and suitability of the hydrothermal conditions. Landscape-level: The landscape connectivity and landscape aggregation indices characterize the integrity and stability of a landscape's spatial structure and the landscape fragmentation index indicates the degree of landscape fragmentation. Park greenspace and green coverage of built-up areas reflect the quality of the human living environment. System-level: Marine aquaculture areas and mineral resource reserves represent the current levels of resource endowment. ③Response indicators reflect deliberate management measures and strategies adopted by society to alleviate pressures, improve adverse conditions, and enhance system adaptability and resilience. Element-level: Habitat quality characterizes coastal biodiversity. Landscape-level:

Environmental governance investment and the marine environmental quality indices represent the effectiveness of economic inputs and policy interventions in regulating the overall coastal environment at the landscape scale. System-level: The area of marine ecological reserves and total number of coastal pollution control projects indicate the capacity for ecological construction and management responses in coastal zones.

Table 2. Indicator system for evaluating the spatial resilience of coastal man–land systems under "element-landscape-system" framework.

Evaluation Object	Element	Landscape	System
Pressure	Human Impact Index E_1[a]	Landscape Pressure Index L_1	Population Growth Rate S_1
			Ecological Pressure Index S_2[b]
			Sea Level Rise Height S_3
State	Ocean Carbon Sequestration E_2	Landscape Connectivity Index L_2	Marine Aquaculture Area S_4
	Water Source Conservation E_3	Landscape Fragmentation Index L_3	Mineral Resource Standard Quantity S_5

	Vegetation Coverage Index E_4	Landscape Aggregation Index L_4	
	Precipitation E_5	Park and Green Space Area L_5	
	Air Temperature E_6	Green Cover in Built-up Areas L_6	
Response	Habitat Quality E_7	Environmental Governance Investment Rate L_7	Marine Ecological Reserve Area S_6
		Marine Environmental Quality Index L_8	Total Coastal Pollution Control Projects S_7
Comprehensive Indicators	Element-level Spatial Resilience E_8	Landscape-level Spatial Resilience L_9	System-level Spatial Resilience S_8

[a]Human Impact Index: $E_1=\sum_{i=1}^{n} A_i w_i/TA$, where A_i denotes the area of the *i*-th land use type, $w_i$represents the parameter reflecting the intensity of human activity disturbance for the *i*-th land use type, *TA* indicates the total area of land use types within the evaluation unit, and *n* is the number of land use types.

[b]Ecological Pressure Index: $S_2 =\sum Ss_i y_i$, where *i* represents the discharge volume of chemical oxygen demand (COD), petroleum hydrocarbons, ammonia nitrogen, and

369 total phosphorus from direct marine discharges in coastal provinces; Ss_i denotes the
370 standardized range value; γ_i is the weighting factor [42].

371 Sensitivity analysis was conducted to evaluate the robustness of the model. After
372 introducing a 20% random perturbation to each indicator, the Pearson correlation
373 coefficient between the original and perturbed results was 0.9997 ($P < 0.001$), and the
374 mean absolute percentage error was approximately 1.07%. These results indicate that
375 spatial resilience was only weakly affected by fluctuations in the input data,
376 demonstrating the high robustness and reliability of the model.

377

378 Research methods

379 Ecosystem service assessment methods

380 (1) Carbon Stock. Carbon stock was assessed using the Carbon module of the
381 InVEST model, which calculates aboveground biomass carbon density, belowground
382 biomass carbon density, soil carbon density, and dead organic matter carbon density
383 [43]. The formulae are as follows:

384 $$C=C_{above}+C_{below}+C_{soil}+C_{dead} \quad (1)$$

385 Where C is total carbon stock (t/hm^2), C_{above} is above-ground carbon stock (t/hm^2),
386 C_{below} is below-ground carbon stock (t/hm^2), C_{soil} is soil carbon stock (t/hm^2), and C_{dead}
387 is dead organic matter carbon stock (t/hm^2).

388 (2) Water Conservation. Water yield was estimated using the Water Yield module
389 of the InVEST model. The annual water yield for each grid cell is given by:

390 $$Y_{jx}=1-(AET_x \div P_x) \quad (2)$$

$$AET_x \div P_x = (1+\omega_x \times R_{xj}) \div (1+\omega_x \times R_{xj} + \frac{1}{Rxj}) \quad (3)$$

$$\omega_x = Z \times AWC_x \div P_x \quad (4)$$

$$R_{xj} = K_{xj} \times ET_x \div P_x \quad (5)$$

Where Y_{jx} is annual water yield, AET_x is annual average evapotranspiration, P_x is annual average precipitation, ω_x is the ratio of modified annual available water to precipitation, R_{xj} is the aridity index, Z is the Zhang coefficient [44], AWC_x is soil available water content, K_{xj} is the vegetation evapotranspiration coefficient, and ET_x is reference crop evapotranspiration.

(3) Habitat Quality. Habitat degradation is first calculated by integrating the sensitivity of different land—use types to threat sources with the external intensity of those threats; habitat quality indices are then derived to quantify habitat status within the study area [45]. The formula is as follows:

$$Q_{xj} = H_j(1 - \frac{D_{xj}^Z}{D_{xj}^Z + K^Z}) \quad (6)$$

Where Q_{ij} is the habitat quality index for grid cell x within habitat type j, H_j is ecological suitability,and Z and K are model default parameters, typically set to 2.5 and 0.5, respectively.

Getis-Ord Gi* Hotspot Analysis

By integrating the characteristics of the available datasets, spatial data-mining methods based on hotspot analysis were used to examine the spatial resilience of man–land systems at the elemental and landscape levels for 1990, 2000, 2010, and 2020. A local spatial autocorrelation analysis was conducted using the Getis-Ord Gi^* statistic on the comprehensive resilience evaluation results, producing distribution maps of

statistically significant hotspots and cold spots. To analyze the spatiotemporal dynamics, hotspots were classified according to the *Gi_Bin* values and combined with four-period raster change information to identify persistent, newly emerging, weakened, and oscillating hotspots.

SHAP Model

SHAP was employed to investigate the nonlinear interactions among the factors influencing the spatial resilience of man–land systems. Traditional linear models have difficulty in capturing complex nonlinear relationships between variables, whereas conventional machine learning models often suffer from “black-box” problems. SHAP overcomes this limitation by combining strong predictive performance with high interpretability, providing both global feature importance and local explanations at the individual sample level [46].

For data processing and parameter tuning, the dataset was randomly split into training and testing sets in an 8:2 ratio. Bayesian optimization was applied to tune the core hyperparameters, and the model performance was evaluated using *K*-fold cross-validation (K = 5), which was chosen to balance the model stability, accuracy, and computational efficiency, given the sample size. During cross-validation, the training set was partitioned into five subsets; in each iteration, four subsets were used for training and one for validation. After five iterations, the optimal parameters for each model were selected based on the cross-validation performance. For the XGBoost model, the optimal hyperparameters were: learning rate (eta) = 0.0136, maximum tree depth (max_depth) = 10, minimum loss reduction (gamma) = 1.53 × 10-7, subsample

ratio (subsample) = 0.519, column subsample by node (colsample_bynode) = 0.4, and minimum child weight (min_child_weight) = 2. The performance evaluation showed that XGBoost achieved a root mean square error (RMSE) of 0.0091 and an (R^2) of 0.9981. Its prediction accuracy, stability, and generalization performance surpassed those of both the Random Forest model (RMSE = 0.0179, (R^2) = 0.908) and Multilayer Perceptron models (RMSE = 0.0312, (R^2) = 0.849). Compared with the Random Forest and Multilayer Perceptron models, XGBoost-SHAP not only retains the superior capability of XGBoost in accurately capturing nonlinear interactions within high-dimensional data, but also realizes the quantification of global feature importance, visualization of factor contributions at the local sample level, and identification of nonlinear threshold effects simultaneously through Shapley value decomposition. This effectively overcomes the limitation of traditional machine learning models that "achieve high prediction accuracy but lack interpretability".

Spatiotemporal evolution

Spatiotemporal evolution of spatial resilience in coastal man–land systems at the element level

Using the natural break method, the element-level evaluation results were classified into four grades of resilience: weak, relatively weak, relatively strong, and strong (Figs 4 and 5). Spatially, the element-level spatial resilience of man–land relations is higher in the north and lower in the south, which closely aligns with the regional development gradient along the southeastern coastal region. Temporally, it

457 shows a complex evolution process characterized by “fluctuating optimization and
458 stepwise upgrading.” The proportion of higher-level resilience areas (relatively strong
459 and strong) remained consistently high, exceeding 61% from 1990 to 2020.

460 In terms of spatial transitions, the resilience of the pressure dimension shows a
461 pattern of “fluctuating bidirectional transfer,” vividly reflecting the geographical
462 dynamics between human development activities and ecological constraints. Guided by
463 strategies such as the development of the Pearl River Delta and the eastern Guangdong
464 port cluster, traditional high-development zones have experienced accelerated port-
465 oriented industrial expansion and land reclamation, resulting in continuous increases in
466 human impact indices and pushing some areas into the weak-resilience category. In
467 contrast, key ecological nodes along the Zhejiang and Fujian coasts effectively curbed
468 negative human disturbances through measures such as the marine ecological redline,
469 mangrove restoration, and “returning farmland to the sea” projects. These interventions
470 enabled areas with previously weak resilience to recover and shift toward moderately
471 strong or strong resilience. The spatial resilience of the state dimension exhibited
472 pronounced stage-dependent fluctuations. In 2010, the proportion of areas with strong
473 resilience declined to 8.99%, whereas the proportion of areas with weak resilience
474 increased to 40.46%. This shift was largely driven by the transmission effects of high-
475 intensity developmental pressures, leading to short-term degradation of natural habitats
476 under intensified human activity. Subsequently, the state dimension exhibited a gradual
477 recovery trend, with the proportion of strongly resilient areas remaining at 21.47%. By
478 contrast, spatial resilience in the response dimension remained relatively stable, with

only minor fluctuations across the resilience categories. Overall, spatial resilience of the man–land system at the element level followed a trajectory of "fluctuating recovery and gradual improvement." Ecological conservation and restoration projects, such as mangrove restoration and coastal zone remediation, have produced clear localized benefits. However, the spatial differentiation pattern of "higher resilience in the north and lower resilience in the south" remains entrenched due to regional development gradients. Ongoing high-intensity human activity pressures in densely developed southern coastal areas continue to represent the core challenge to further improve the overall spatial resilience.

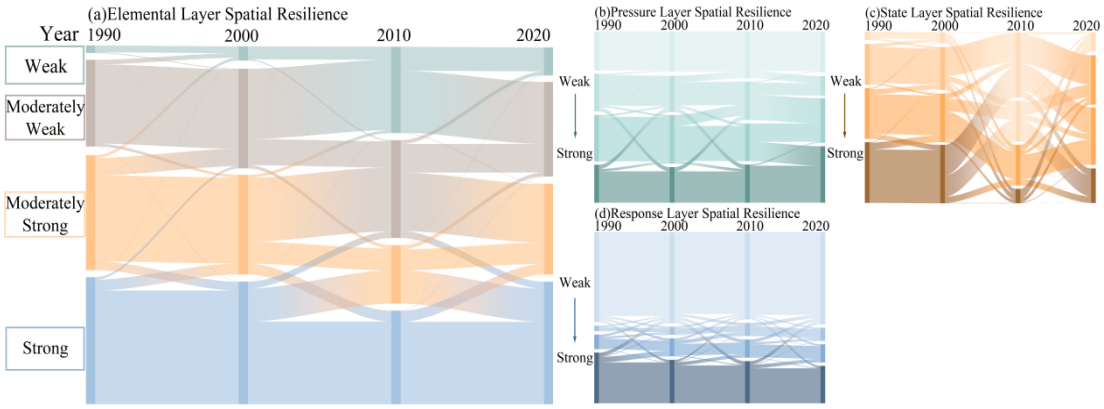

Fig 4. Areal variation of spatial resilience in each dimensional space

Fig. 5e shows that resilience hotspots and cold spots in the man–land system follow a pattern of "hotspots clustering in the north and cold spots expanding along the southern edge." From 1990 to 2020, hotspots expanded at 54.97 km²/yr (0.09%/yr intensity), while cold spots contracted slightly at 41.07 km²/yr (0.07%/yr intensity), indicating a slow but positive overall trend. Phased changes are evident: From 1990 to 2000, early conservation gains: Hotspots expanded rapidly (176 km²/yr, 0.30%/yr), and cold spots contracted markedly (216.1 km²/yr, −0.39%/yr). Ecological control began in

the north, whereas southern development pressures remained fragmented, reflecting the initial success of conservation. Between 2000 and 2010, rising development pressure: Policy priorities shifted toward rapid growth, accelerating industrialization and urbanization along the southeastern coastal region. Industrial clustering in the Pearl River Delta and port expansion in eastern Guangdong intensified pressures, causing hotspots to contract (116.5 km^2/yr, 0.19%/yr) and cold spots to expand in the short term (183.5 km^2/yr, 0.35%/yr). From 2010 to 2020, in the ecological restoration phase, national measures such as the Marine Ecological Redline System and coastal zone management were implemented intensively. Restoration efforts renewed hotspot expansion (105.4 km^2/yr, 0.18%/yr), while cold spots returned to contraction (90.6 km^2/yr, 0.17%/yr). Spatially, persistent and oscillating hotspots clustered along the central-northern Zhejiang and northeastern Fujian coasts, where stronger aggregation and reduced extent formed stable high-value zones. Persistent and oscillating cold spots extend from the Pearl River Delta to the eastern Guangdong coastline, with some diffusion toward nearby inland nearshore areas. This pattern reflects functional zoning under the “northern conservation and southern development” strategies along the southeastern coastal region. The three main drivers underlying these patterns are: (1) ecologically reinforced zones, where redline controls and wetland/mangrove conservation further strengthen the already strong-resilience; (2) low-disturbance sustained zones, which maintain moderately strong-resilience over the long term due to solid ecological baselines and topographic constraints; and (3) ecologically restored transition zones, which improve resilience through “farming-to-sea conversion” and

519 “coastal restoration projects.” Cold spot expansion is concentrated in the Pearl River
520 Delta and eastern Guangdong, where intensive port construction, port-adjacent
521 industrial clusters, and land reclamation impose persistent pressures. Despite
522 interventions, development-conservation conflicts remain pronounced, making these
523 areas priorities for future resilience enhancement.

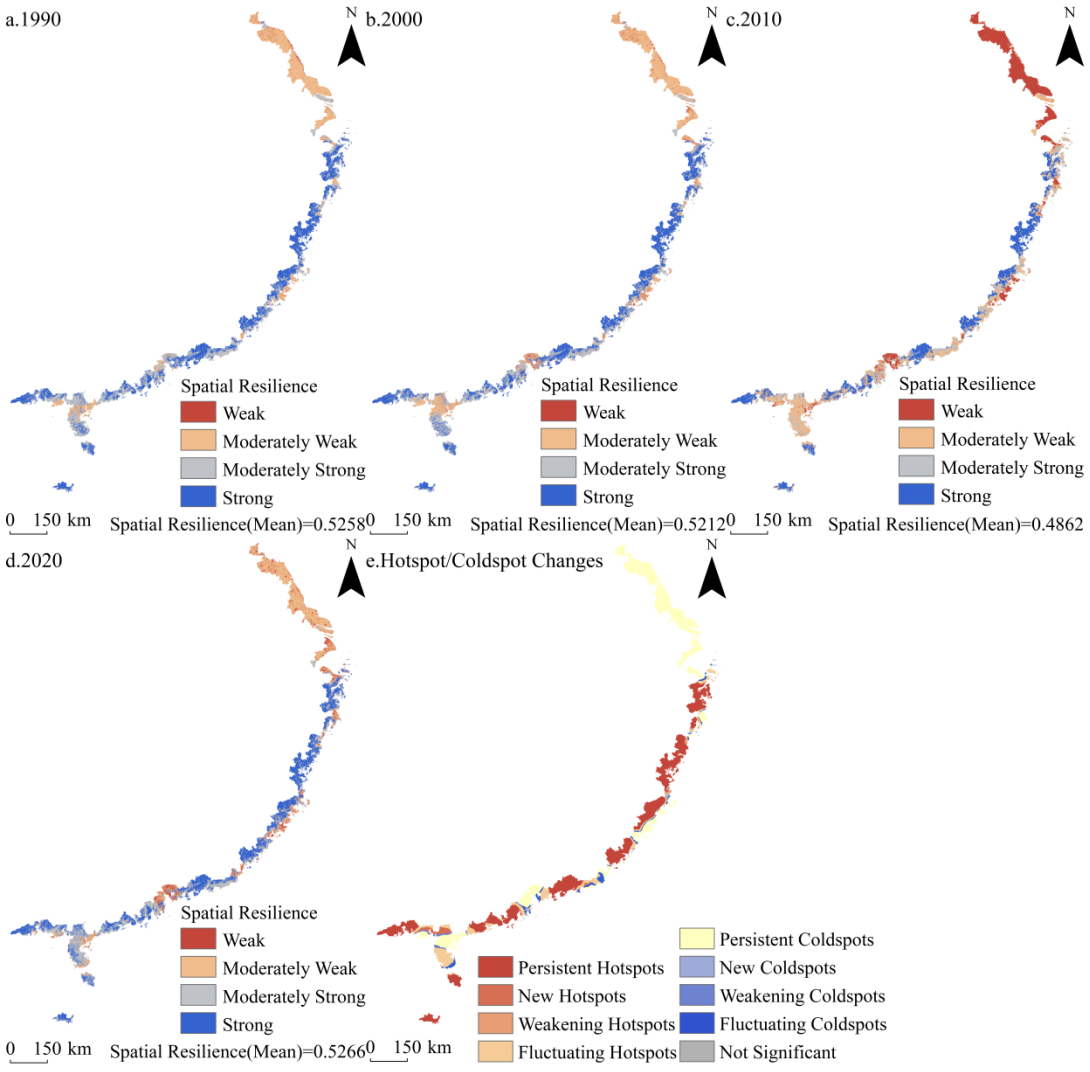

524

525 Fig 5. Spatial and temporal change of the spatial resilience of the man–land regional
526 system at the element level during 1990-2020

527

Spatiotemporal evolution of spatial resilience in coastal man–land systems at the landscape level

Using the natural breakpoint method, the landscape-level evaluation results were categorized into four resilience levels: weak, moderately weak, moderately strong, and strong (Figs 6 and 7). Spatially, the overall distribution pattern can be summarized as "higher resilience in northern coastal areas and lower resilience in southern bay areas, with clustered resilience on eastern islands and differentiated resilience along western coastlines." Temporally, it exhibits a progressive evolution characterized by a "dominance of medium-low grades and contraction of high grades." The proportion of medium-low (weak and moderately weak) resilience areas remained consistently above 63%, whereas the proportion of strong resilience areas declined markedly from 9.85% in 1990 to 5.49% in 2020. Overall, the pattern converged toward "clustering of moderately weak grades and weakening of strong grades."

In terms of spatial dynamics, the study period witnessed a "weak-strong oscillation" in spatial resilience across the pressure layers. Driven by coastal industrial expansion, port construction, and other development activities, some areas experienced surging development intensity, accelerated landscape fragmentation, and rising human footprint indices, pushing spatial resilience toward the weak category. At the same time, supported by ecological initiatives such as negative lists of coastal development, land reclamation controls, and mangrove restoration, other regions effectively curbed adverse human disturbances, enabling some areas with weak resilience to recover to stronger resilience levels. The spatial resilience pattern in the state layer remains

relatively stable. Long-term maintenance of coastal protective forests and mangrove ecosystems has maintained relatively steady-state indicators, such as landscape connectivity and habitat quality. Although the proportion of areas with strong resilience areas was low overall, it remained stable without pronounced fluctuations. However, because of historical legacy issues, such as shoreline hardening and habitat fragmentation, compounded by potential climate-induced disturbances to coastal landscapes, the proportion of weak and moderately weak resilient areas has declined only gradually, without fundamentally altering the core spatial pattern. The response layer exhibits “gradient differentiation and localized optimization.” In some areas, targeted initiatives such as “returning farmland to the sea” and “mangrove afforestation,” have accelerated the transition from weak to stronger resilience levels. By 2020, the proportion of areas with weak resilience had decreased by 6.36 percentage points compared to 1990, indicating gradual progress in restoration. Nonetheless, owing to developmental inertia, the increase in strongly resilient areas has remained sluggish, failing to reverse the overall decline in higher resilience levels. Overall, the spatial resilience of the man–land system at the landscape level exhibits a pattern of “overall degradation with localized optimization.” Although ecological restoration projects have achieved localized improvements, the persistent decline in resilience remains unresolved. Ongoing pressures from intensive development and historical ecological deficits continue to be core constraints on the overall enhancement of resilience.

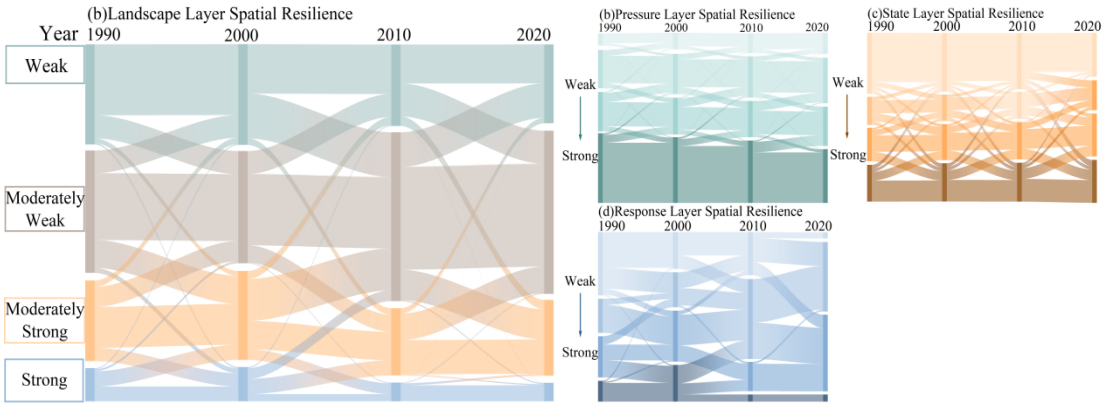

Fig 6. Areal variation of spatial resilience in each dimensional space

Fig 7e shows that spatial resilience hotspots and cold spots of the man–land system in the landscape layer, exhibit a pattern in which hotspots cluster along the northern section, whereas cold spots expand in a belt-like form along the southern bay. From 1990 to 2020, hotspots contracted at a rate of -623 km^2 /yr (-0.67%/yr intensity), whereas cold spots expanded at 416.17 km^2 /yr (0.27%/yr intensity). This reflects an overall degradation trend in landscape-level resilience, indicating that ecological conservation efforts have not been sufficient to offset developmental pressures. Phase analysis revealed distinct stages. From 1990 to 2000, hotspots expanded and cold spots contracted: hotspot areas grew at 1,025.7 km^2/yr (1.12%/yr intensity), while cold spots contracted at -1,700.3 km^2/yr (-1.12%/yr intensity). Initial ecological controls in the north produced visible conservation gains on islands and coastlines, strengthening hotspot clustering effects. Between 2000 and 2010, an abrupt contraction of hotspots and expansion of cold spots occurred, with hotspot areas shrinking at -1,722.8 km^2/yr (-1.67%/yr intensity) and cold spot areas expanding at 554.2 km^2/yr (0.41%/yr intensity). Development intensity surged in the south, causing northern hotspots to

shrink under increasingly diffusing development pressures and substantially offsetting earlier conservation benefits. From 2010 to 2020, hotspots continued to contract while cold spots accelerated their expansion: hotspot areas decreased at -1,171.9 km²/yr (-1.37%/yr intensity), and cold spot areas expanded at 2,394.6 km²/yr (1.70%/yr intensity). Intensified development pressures in the south drove cold spots to spread contiguously along the bay coast, further reinforcing the degradation trend. Spatially, persistent and newly emerging hotspots were clustered strongly on northern islands such as Zhejiang's Zhoushan Archipelago and Fujian's Pingtan Island, as well as along the coastal areas of Ningde, exhibiting pronounced nucleation effects despite the shrinking spatial extent. Persistent and oscillating cold spots have expanded along the Pearl River Delta coastline and segments of the western Guangdong shoreline, encroaching into nearshore towns and tidal flats. This pattern reflects the spatial projection of an imbalance between development and conservation in northern and southern regions. Hotspot formation is driven by three mechanisms. Island-concentrated hotspots rely on relatively isolated habitats and strict ecological redline controls, where industrial transformation and low human disturbance help maintain strong-resilience. Coastal conservation-driven hotspots enhance resilience from strong to stronger through wetland restoration and the synergy of green development, consolidating the northern hotspot zones. Restoration-driven hotspots improve resilience from weak to strong via measures, such as aquaculture-to-tidal-flat conversion and mangrove afforestation, forming new localized hotspot areas. In contrast, the expansion of cold spots has resulted from the combined effects of intensive

development in the south and long-standing ecological deficits. Despite localized restoration efforts, the tension between development and conservation remains unresolved, making the southern coastal areas key targets for future enhancement of landscape-level resilience.

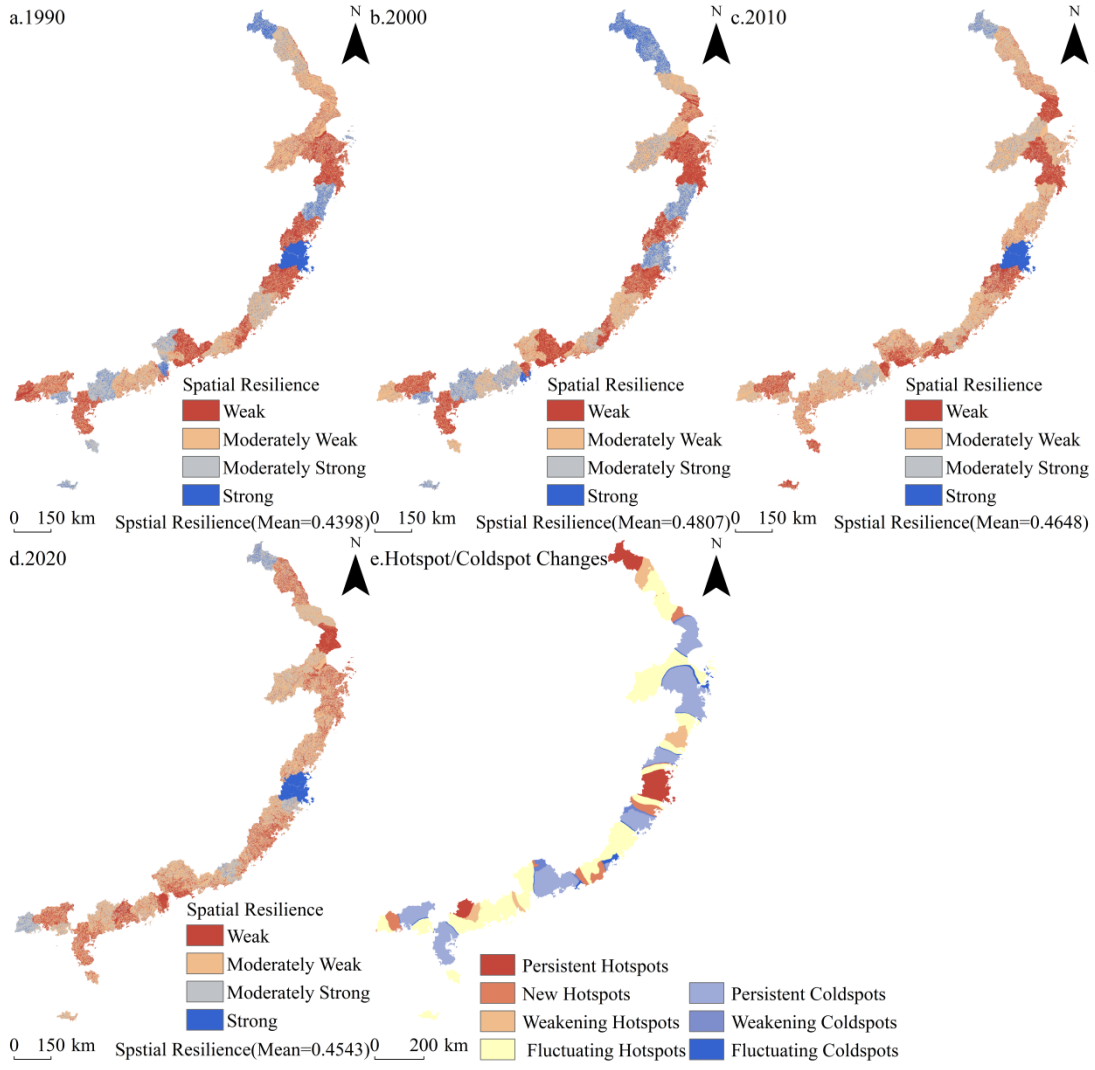

Fig 7. Spatial and temporal change of the spatial resilience of the man–land regional system at the landscape level during 1990-2020

Spatiotemporal evolution of spatial resilience in coastal man–land systems at the system level

Based on the hierarchical results of the natural breakpoint method, the spatiotemporal evolution of spatial resilience at the system-level exhibits distinct characteristics (Fig 8). Temporally, it follows a pattern of “initial increase, subsequent decline, and then fluctuation.” While spatially, it is characterized by “stronger resilience in the north, weaker in the south, with localized oscillations.” From 1990 to 2000, average spatial resilience increased from 0.4479 to 0.4922. Along the Zhejiang and Fujian coasts, favorable ecological foundations—such as subtropical coastal wetlands and mangrove ecosystems—combined with an early policy orientation of “moderate development with priority on conservation” in the National Marine Development Plan, maintained relatively low development intensity and a stable proportion of strong-resilience areas. In the southern Pearl River Delta, the overall scale of development was constrained by the early stages of an export-oriented economy, resulting in limited human disturbance of coastal habitats. Regional resilience showed a gradual upward trend, with scattered weakly resilient patches appearing on some islands due to disorderly traditional aquaculture. From 2000 to 2010, the average spatial resilience decreased to 0.4526. Northern Zhejiang and coastal Fujian generally retained strong resilience, supported by coastal development controls and ecological redline demarcations. In contrast, the southern Pearl River Delta is under increasing pressure from port-cluster construction and port-adjacent industrial agglomeration, as promoted by the Outline of the Pearl River Delta Region Reform and Development Plan (2008–2020). Port expansion and the growth of industrial land in areas such as Nansha (Guangzhou) and Bao’an (Shenzhen) have intensified habitat fragmentation. Weak-

resilience areas are spread along coastal belts, and some islands are affected by cross-regional fishery pollution, leading to concurrent declines in resilience and a reduction in the regional average. From 2010 to 2020, the average spatial resilience decreased slightly to 0.4510. Along the Zhejiang and Fujian coasts, implementation of the National Marine Ecological Civilization Construction Implementation Plan—through initiatives such as “Blue Bay” remediation and large-scale mangrove restoration—concentrated strong-resilience areas. In the southern region, although development inertia allowed weak-resilience patches to continue encroaching toward the coastline, enforcement of the Measures for the Control of Land Reclamation and Filling and the Guangdong-Hong Kong-Macao Greater Bay Area Ecological Environment Protection Plan helped arrest the continuous decline in resilience. These policies established a dynamic equilibrium between development pressures and regulatory interventions through measures such as returning farmland to tidal flats and shoreline restoration.

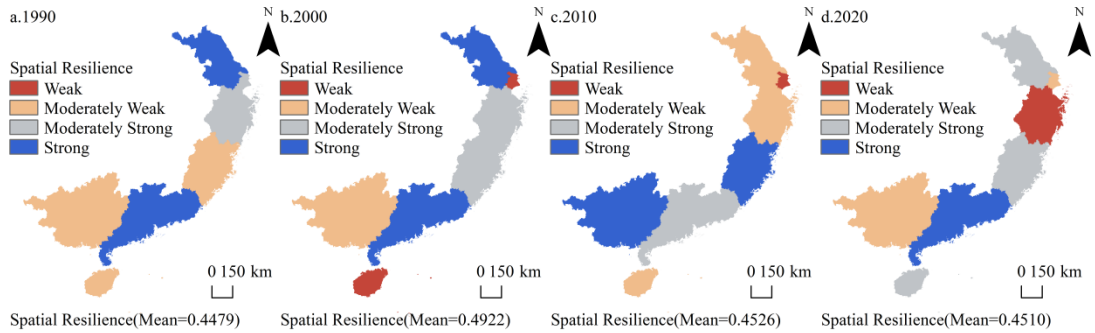

Fig 8. Spatial and temporal change of the spatial resilience of the man–land regional system at the system level during 1990-2020

Influencing factors

Feature importance

Fig 9 shows the relative importance of the variables influencing spatial resilience at element, landscape, and system levels. At the element level, habitat quality (35.17%) had the highest relative importance, followed by the human impact index (23.86%), and marine carbon sequestration (23.37%), underscoring the central role of ecological foundation elements in supporting and regulating resilience in the man–land system. Water conservation, climate-related factors (precipitation and temperature), and the vegetation coverage index exert comparatively weaker influences on element-level resilience. At the landscape level, landscape pattern characteristics and regulation of human activity jointly constitute the primary drivers of resilience. Among these, the landscape connectivity index (29.24%) and built-up area greening coverage (26.55%) were particularly influential, whereas variables such as environmental governance investment, park green space area, and the landscape pressure index also contributed to landscape-level resilience. The landscape fragmentation, landscape aggregation, and marine environmental quality indices have relatively limited effects on landscape scale spatial resilience. System-level analysis showed that socio-economic pressure factors, marine resource utilization, and ecological protection collectively dominated the changes in spatial resilience. Within this group, marine aquaculture area (28.87%) and natural population growth rate (22.22%) exhibited the highest relative importance. The effects of the mineral resource standard volume (9.12%), total number of coastal pollution control projects (5.77%), and ecological pressure index (5.63%) on system-level resilience were relatively weak.

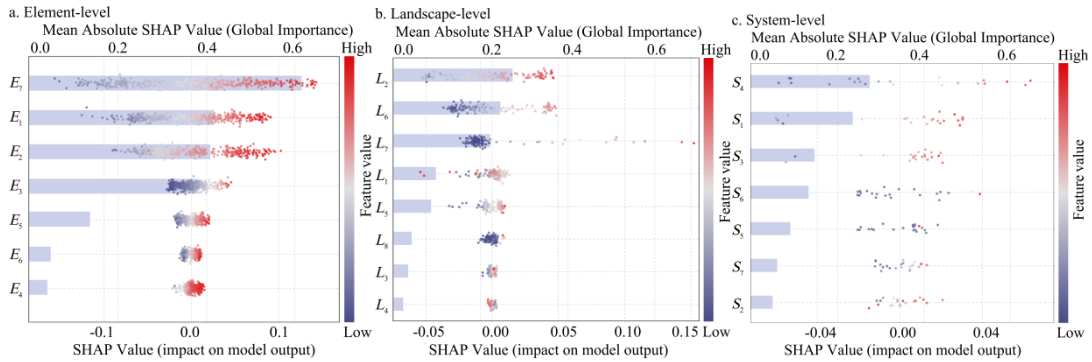

Fig 9. Summary of the characteristics importance of variables of spatial resilience in coastal man–land systems: Based on SHAP analysis

Nonlinear effects and threshold effects

Partial dependency plots and threshold detection results indicated that all variables showed significant nonlinear characteristics and threshold effects on the spatial resilience of the man–land system. At the element level, spatial resilience is driven by "ecological baseline dominance with auxiliary regulation by human and climatic factors" (Fig 10). The ecological baseline variables were the core support for spatial resilience, showing stable influencing trends with clear thresholds. Habitat quality had a monotonically positive effect on resilience, with a threshold of 0.69. Above this value, the system is vulnerable and has limited regulatory capacity. Above this value, biodiversity maintenance and self-repair markedly improve, forming a virtuous cycle. Water conservation (threshold 0.26) and marine carbon sequestration (threshold 0.35) show "increasing marginal benefits" and "saturation effects," respectively. Once the water conservation threshold is exceeded, basin hydrological regulation and ecological water replenishment increase significantly, which is consistent with the concentrated precipitation and hydrologically sensitive coastlines in the southeast coastal region. Marine carbon sequestration levels off after this threshold, reflecting the upper limit of

the ecological carrying capacity for carbon-sequestering vegetation such as mangroves and salt marshes. Human activities and climatic factors act as auxiliary regulators with a relatively limited overall influence. The human impact index displays a complex pattern: below 0.60, moderate human activities (e.g., rational aquaculture and eco-tourism) slightly enhance resilience; above this threshold, intensive activities such as land reclamation and industrial pollution reduce the restoration capacity and cause a continuous decline in resilience, mirroring man–land conflicts under rapid industrialization and urbanization on the southeast coastal region. Among climatic factors, precipitation shows an “optimal moderate” pattern. Below 0.70, water scarcity constrains resilience improvement; above it, issues such as shoreline erosion and wetland flooding may occur, which is consistent with the uneven spatiotemporal distribution of precipitation under the monsoon climate of the southeastern coastal region. Temperature and vegetation coverage index exerted relatively gradual effects on spatial resilience.

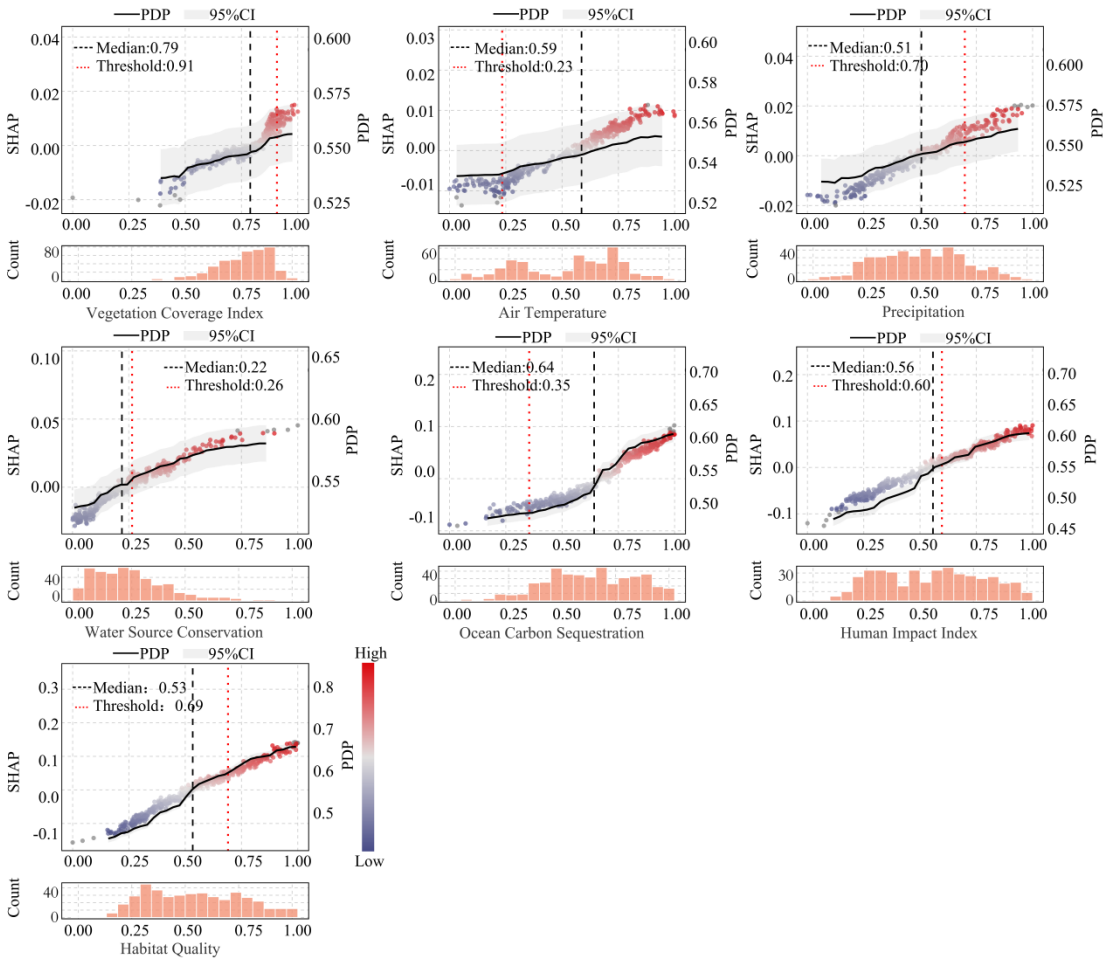

Fig 10. Partial dependence analysis of the element level

At the landscape level, which is distinct from the elemental level, with an emphasis on ecological foundation support, the focus is on an intermediate scale linking micro-ecological processes to macro-spatial patterns. At this scale, the influence of key variables on the spatial resilience of man–land systems was characterized by “human regulation dominance and spatial configuration coordination” (Fig 11). Environmental governance investment is a key regulatory variable on this scale. It has a 0.67 threshold with a narrow 95% confidence interval, indicating a stable effect. Below 0.67, the SHAP values remained low, indicating that underinvestment in pollution control

facilities prevents economies of scale and constrains collaborative environmental governance. Above 0.67, the SHAP values increased sharply, implying that centralized, large-scale investments can effectively reduce pollution from industrial clusters and dense port areas in southeastern coastal cities, improving both ecological environmental quality and system resilience. The landscape pressure index has a threshold of 0.91 and exhibits a “critical constraint” effect. Below 0.91, SHAP values are near zero, indicating that development intensity generally remains within the ecosystem carrying capacity and landscape integrity is maintained. Beyond 0.91, SHAP values became negative and their absolute values grew as confidence intervals narrowed, indicating escalating disruption of landscape connectivity and irreversible damage to ecological corridors from activities such as land reclamation and the expansion of construction land. Among the landscape pattern variables, the landscape connectivity and landscape aggregation indices displayed strong threshold effects related to the spatial distribution of wetlands and coastlines along the southeastern coastal region. When the connectivity was below 0.77, the Partial Dependence Plot (PDP) curve was flat, reflecting weak links between habitat patches, constrained species movements, and ecological processes. Above 0.77, the curve becomes steep, indicating that continuous landscape corridors markedly enhance disturbance resilience and material cycling efficiency. The landscape aggregation index shows an “optimal moderation” effect: moderate aggregation supports ecological clustering and efficient resource use, whereas excessive aggregation can cause local ecological overload. This aligns with the fragmented patch structure and artificially interspersed natural landscapes typical of the southeastern

coastal region. In contrast, variables such as the marine environmental quality index and park green space area showed moderate threshold effects, whereas the wide 95% confidence intervals for the landscape fragmentation index and built-up area with green coverage indicated relatively weak threshold behavior.

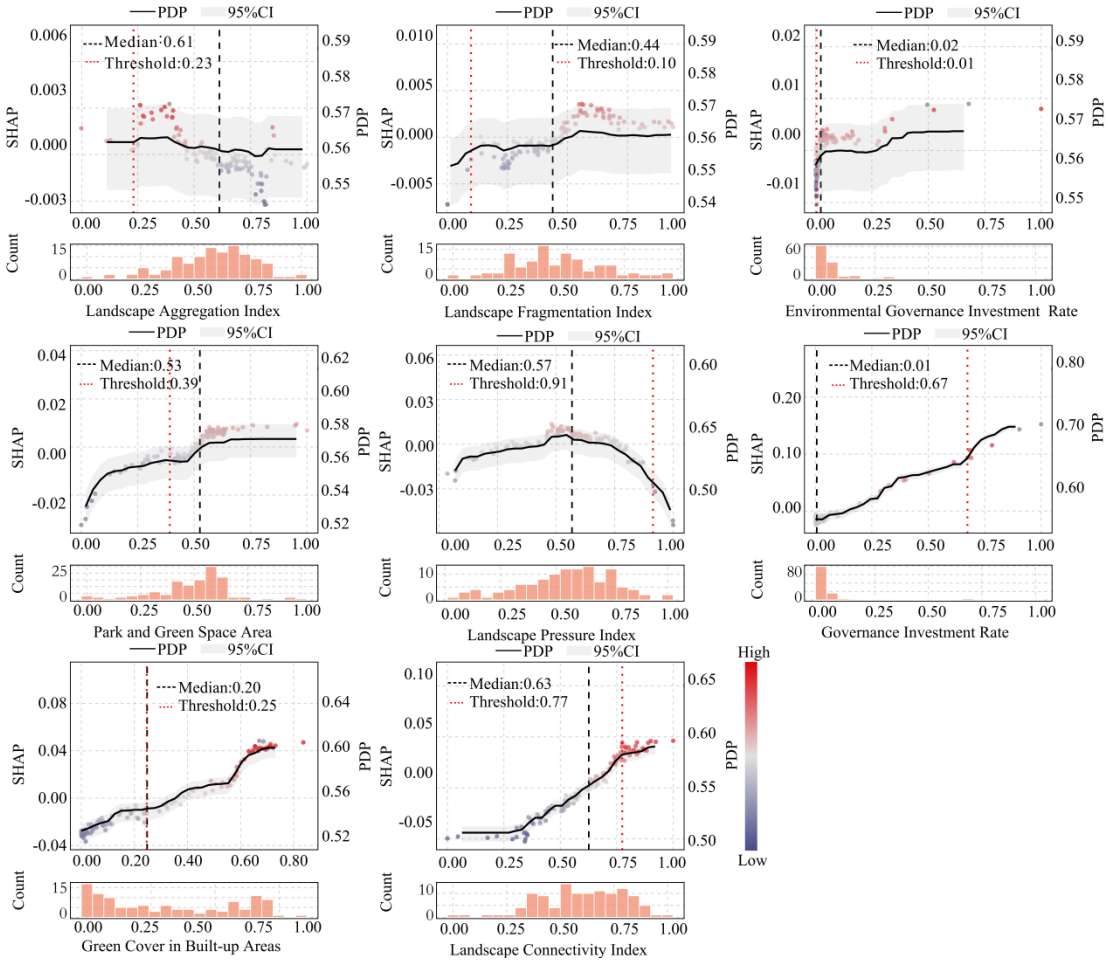

Fig 11. Partial dependence analysis of the landscape level

As a key scale linking micro-ecological processes and macro-regional development, system-level variables exert a dual influence on the spatial resilience of man–land systems in the southeastern coastal provinces: a “resource utilization versus ecological conservation trade-off” and a “synergy between socio-economic pressures

and ecological regulation" (Fig 12). Two variables, natural population growth rate and marine aquaculture area, are particularly important, exhibiting marked threshold effects. The natural population growth rate showed a strong negative nonlinear effect on resilience, with a threshold of 0.54. Below this threshold, the negative contribution of SHAP values is relatively weak, implying that population growth pressures remain within the regional resource-environment carrying capacity and can be buffered through system self-regulation. Above this threshold, negative SHAP values effect significantly increased. Under conditions of high population concentration and dense urbanization in the southeastern coastal provinces, continued population growth leads to resource depletion and spatial crowding that surpasses the ecological carrying capacity such that self-regulatory mechanisms can no longer offset the resulting negative impacts. The marine aquaculture area has a threshold at 0.07, displaying a nonlinear "ecological benefits first" pattern. Below this threshold, the positive contribution of SHAP values was minimal, suggesting that moderate aquaculture can balance economic returns and ecological effects. Beyond the threshold, the PDP curve rose steeply in the negative direction, and the SHAP values became strongly negative. This indicates that the adverse effects of large-scale aquaculture, such as water pollution and habitat degradation, override its economic benefits and cause a sustained decline in system resilience. The ecological pressure index had a threshold of 0.95. Below this value, the PDP curve is relatively flat and the SHAP values are close to zero, indicating that the pressures from industrial expansion and human activity intensity remain generally manageable. Above this threshold, the curve steepens, the negative impacts

increase substantially, and the 95% confidence interval narrows, reflecting the cumulative structural damage to ecosystems caused by overlapping pressures. This pattern is consistent with the accumulation of ecological stress under rapid industrialization and urbanization in southeastern coastal provinces. In comparison, the threshold effects associated with the marine ecological reserve area, sea-level rise height, mineral resource standard volume, and total number of coastal pollution control projects are relatively moderate, with lower impact intensity on system resilience.

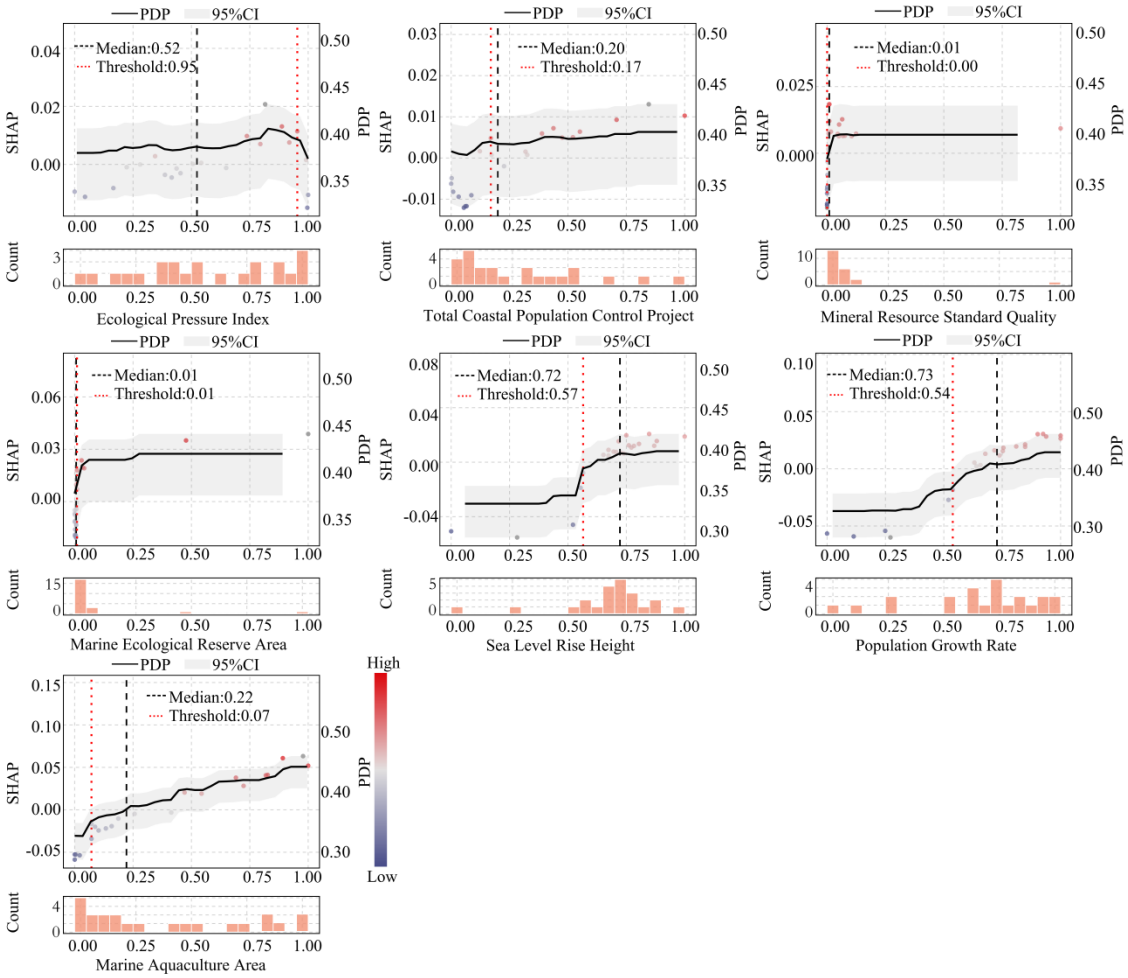

Fig 12. Partial dependence analysis of the system level

Conclusions

Taking the southeastern coastal region as a case study, this study elucidates the spatial resilience of man–land systems at the macro-, meso-, and micro-scales. An evaluation framework for coastal man–land system resilience is constructed based on the "element-landscape-system" framework. Hotspot analysis was employed to examine the spatiotemporal evolution of resilience, whereas machine learning models and SHAP visualization was used to identify influencing factors and their patterns. Key findings include:

(1) Overall, the spatial resilience of the southeastern coastal region man–land system improved gradually, with clear spatiotemporal differences across scales. At the element level, resilience is "higher in the north, lower in the south," with "northern hotspot clusters and expanding southern cold spots." At the landscape level, hotspots are concentrated on the northern coastal islands (e.g., the Zhoushan Archipelago and Pingtan Island), whereas cold spots form a belt along the Pearl River Delta Bay coast. At the system level, resilience follows a pattern of "strong in the north, weak in the south, with local oscillations." Strong-resilience areas such as Zhejiang and Fujian continued to cluster, whereas weak-resilience areas in the south showed no fundamental shift in spatial patterns.

(2) XGBoost and SHAP analyses showed that the drivers of coastal man–land resilience were clearly scale-dependent. At the elemental level, ecological baselines dominated, with habitat quality and the human impact index contributing 35.17% and 23.86%. At the landscape level, human activity regulation and landscape configuration prevailed, with landscape connectivity and green coverage of built-up areas

814 contributing 29.24% and 26.55%, respectively. At the system level, socio-economic
815 pressure and marine resource use dominate, with marine aquaculture area and natural
816 population growth contributing 28.87% and 22.22%. This scale-progressive influence
817 mechanism reveals intrinsic patterns in the human–sea system complexity.

818 (3) High-contributing variables exhibited marked threshold effects on spatial
819 resilience. Similar variables at the same scale shared convergent thresholds, indicating
820 common rules for enhancing ecosystem services. The thresholds differ significantly
821 across scales because of variations in the spatial scope and functional roles of the
822 evaluated objects, leading to different system sensitivities and tolerance limits. Thus,
823 regulating the spatial resilience of coastal man–land systems require differentiated,
824 scale-specific threshold control strategies.

825

826 Discussion

827 Based on the above analysis, the following zoning management strategies are
828 proposed: (1) Strong resilience consolidation zones: Zhejiang should strictly enforce
829 ecological redlines in areas such as the Zhoushan Archipelago and Wenzhou Bay, ban
830 new land reclamation, restore contiguous mangrove forests, and build coastal wetland
831 ecological networks. Around the Ningbo-Zhoushan Port area, the landscape
832 configuration should be optimized, improve compatibility between industrial land and
833 ecological space, and include habitat quality and landscape connectivity in performance
834 evaluations. Fujian should use the “Blue Bay” remediation project to strengthen island
835 ecological corridors, strictly control offshore aquaculture scale, and promote ecological

upgrading of aquaculture zones. (2) Moderately resilient enhancement zones: Shanghai should restore coastal wetlands in the Yangtze River estuary, renovate ecological shorelines, enhance connectivity between parks, green spaces, and coastal corridors, strengthen integrated land–sea pollution control, and balance port-adjacent industrial development with ecological conservation. Jiangsu should address the degradation of coastal tidal flats by reducing aquaculture, replenishing ecological water, and improving wetland hydrological regulation. It should optimize the coastal industrial layout, promote the green and low-carbon transformation of port-related industries, and reduce landscape fragmentation caused by development. Southern Fujian should establish cross-county ecological protection mechanisms to address port development pressures in Xiamen Bay and Quanzhou Bay, optimize “patch-corridor-matrix” spatial patterns, and strengthen the disturbance resilience of bay ecosystems. (3) Moderate resilience improvement zones: Hainan must strictly enforce ecological protection redlines, limit the density of coastal tourism projects, restore damaged shorelines and mangroves and enhance water conservation and habitat quality. Eastern Guangdong should address aquaculture pollution and landscape fragmentation along the Shantou and Shanwei coasts by upgrading pollution control facilities, promoting the advanced treatment of industrial wastewater, phasing out inefficient aquaculture, and improving the ecological base through afforestation and wetland water replenishment. (4) Weak resilience challenge zones: The Pearl River Delta region of Guangdong should deepen ecological governance coordination within the Guangdong-Hong Kong-Macao Greater Bay Area, relocate high-polluting enterprises from the Pearl River Estuary, implement

zero-growth land reclamation policies, restore estuarine wetlands, and establish a closed-loop governance system that links “land-based reduction, coastal buffering, and marine improvement” to reconcile development and conservation. Western Guangdong should control coastal industrial expansion and aquaculture pollution in Zhanjiang and Maoming, build a network of marine ecological protection zones, strengthen land-based pollutant interception and reduction, and promote the large-scale restoration of coastal wetlands and mangroves.

Building on this foundation, further policy recommendations are proposed.

①Policies for removing barriers to factor mobility. Addressing the “strong in the north, weak in the south” spatial pattern identified in this study, a multi-tiered policy system will be implemented to remove obstacles to the flow of ecological, industrial and policy elements across scales. At the element level, cross-regional transfer of ecological compensation funds will be promoted from regions meeting habitat quality thresholds (≥0.69), and a “north protects, south compensates” horizontal compensation mechanism will be established. At the landscape level, landscape connectivity optimization standards for coastal cities (≥0.77) will be unified to break down administrative boundaries fragmenting ecological corridors, facilitating cross-regional integration of ecological elements such as parks, green spaces and wetlands. At the system level, approval procedures for seawater aquaculture, port construction and other projects will be streamlined, and a cross-provincial linkage mechanism between industrial relocation and ecological conservation will be set up to guide capital,

technology and other production factors toward low-disturbance and high-efficiency sectors.

②Synergistic policies for ecological conservation and industrial upgrading. Leveraging the advantages of marine resources, wetland ecosystems and port locations in the southeastern coastal region, and combining spatial resilience thresholds, industrial structure optimization will be promoted in a coordinated manner. In strong-resilience areas, green industries including eco-tourism and marine carbon sinks will be prioritized, integrating mangrove and wetland conservation into blue carbon trading. In moderately strong-resilience areas, circular transformation of port-adjacent industries will be advanced, while industrial development intensity will be strictly controlled below the landscape pressure index threshold (0.91). In moderately weak-resilience areas, inefficient and polluting aquaculture as well as high-energy-consuming industries will be phased out, and the region will shift toward low-disturbance and high-value-added sectors such as seawater desalination and marine biomedicine, so as to achieve a win-win between ecological conservation and economic development.

③Policies for strengthening cross-regional collaborative governance. Focusing on the “strong in the north, weak in the south” spatial pattern revealed in this study, a multi-tiered collaborative governance system will be constructed. At the provincial level, a monitoring and early warning platform for coastal spatial resilience will be built in the southeastern coastal region, with standardized control indicators including ecological pressure index (threshold 0.95) and marine aquaculture coverage (threshold 0.07). At the regional level, ecological joint prevention and control will be deepened

among coastal cities in the Guangdong-Hong Kong-Macao Greater Bay Area and the Yangtze River Delta, with shared pollution monitoring data and coordinated wetland restoration. At the national level, spatial resilience enhancement will be integrated into integrated land-sea development planning; special cross-regional ecological protection funds will be established to support weak-resilience areas in carrying out key projects such as mangrove restoration and pollution control, so as to promote overall regional sustainable development.

The study still has several limitations that require further refinement. First, the indicator system inadequately captures processes unique to the coastal zone. Owing to limited marine spatial data, indicators such as reclamation intensity and shoreline artificialization rate were omitted, which may have reduced the precision of assessing human impacts on nearshore ecosystems. Second, the model assumptions contained potential biases. The study simplifies the “linear relationship between human activities and ecological responses” and the “homogeneity of internal system elements,” which differs from the actual complex nonlinear interactions within ecosystems. Third, spatial unit boundary effects were insufficiently considered. Fixed administrative boundaries do not capture the continuity and integrity of coastal ecosystems and may overlook cross-regional ecological linkages and impact transmission, weakening the explanatory power of resilience evolution from an integrated land–sea perspective.

Acknowledgements

The authors are grateful to the editors and reviewers for their constructive comments and suggestions. The authors also thank all data sources and institutions that provided support for this study.

References

1. Griggs D, Stafford-Smith M, Gaffney O, Rockström J, Öhman MC, Shyamsundar P, et al. Sustainable development goals for people and planet. Nature. 2013;495:305-307.
2. Zhao WW, Yin CC, Zhang JZ, Fu BJ. Progress and prospects of geography in promoting the United Nations Sustainable Development Goals: a discussion on the theoretical framework of sustainable geography. Acta Geogr Sin. 2024;79:2699-2720.
3. Li B. Theoretical, methodological, and empirical studies on the vulnerability and adaptability of the human–sea territorial system. Beijing: Science Press; 2018:64-67.
4. Ferraro PJ, Sanchirico JN, Smith MD. Causal inference in coupled human and natural systems. Proc Natl Acad Sci. 2019;116:5311-5318.
5. Tang YZ, Shi TZ, Liu Q, Wang MD, Yan FQ, Lv P, et al. Ecological carrying capacity and sustainability assessment for coastal and maritime area based on

spatial scene: a case study of the Guangdong-Hong Kong-Macao Greater Bay Area. Acta Geogr Sin. 2023;78:2811-2832.

6. Holling CS. Resilience and stability of ecological systems. Annu Rev Ecol Syst. 1973;4:1-24.
7. Holling CS, Gunderson LH. Resilience and adaptive cycles. In: Gunderson LH, Holling CS, eds. Panarchy: understanding transformations in human and natural systems. London: Island Press; 2002:25-62.
8. Holling CS. Understanding the complexity of economic, ecological, and social systems. Ecosystems. 2001;4:390-405.
9. Su F, Mo XH, Tong L, Zheng K, Cao YR. Progress on adaptability of tourism destination social–ecological system. Sci Geogr Sin. 2020;40:280-288.
10. Fu YC, Guo BY, Wang M, Qin XL. Spatial resilience evolution of green space from the perspective of social–ecological system adaptive governance: a case study for urban renewal in Guangzhou, China. J Nat Resour. 2022;37:2118-2136.
11. Adger WN. Social and ecological resilience: are they related? Prog Hum Geogr. 2000;24:347-364.
12. Frazier TB, Thompson CM, Dezzani RJ, Butsick D. Spatial and temporal quantification of resilience at the community scale. Appl Geogr. 2013;42:95-107.
13. Gunderson L, Holling CS. Panarchy: understanding transformations in human and natural systems. Washington DC: Island Press; 2002:1-536.

14. Cutter SL, Barnes L, Berry M, Burton C, Evans E, Tate E, et al. A place-based model for understanding community resilience to natural disasters. Glob Environ Change. 2008;18:598-606.
15. Cutter SL, Ash KD, Emrich CT. The geographies of community disaster resilience. Glob Environ Change. 2014;29:65-77.
16. Huang T, Wei M, Xi JC. Evolution difference and influence mechanism of social-ecosystem resilience in rural tourism destinations: based on the comparative demonstration of the core-edge areas of the Yangtze River Delta. Sci Geogr Sin. 2024;44:492-501.
17. Ma JH, Chen J, Yang XJ, Zhang XW. Influence of land use change on rural social resilience in arid areas: taking the Minqin Oasis as an example. Resour Sci. 2021;43:1615-1627.
18. Yang XJ, Shi YZ, Wang ZQ. Exploring the impacts of road construction on a local social–ecological system in Qinling mountainous area: a resilience perspective. Acta Geogr Sin. 2015;70:1313-1326.
19. Zhang M, Zhou Y, Sang S. Vulnerability analysis of the economic-social-ecological complex system of Island tourism destinations. PLoS ONE. 2025; 20(7): e0324714. doi: 10.1371/journal.pone.0324714.
20. Jin QH, Wang QM, Li Y, Li YF. Evaluation of landscape connectivity in China's coastal terrestrial nature reserves based on an improved minimum cumulative resistance model. Acta Geogr Sin. 2021;76:2830-2840.

21. Zhang X, Liang XY, Liu D, Shi QQ, Chen H. The resilience evolution and scenario simulation of social–ecological landscape in the fragile area. Acta Geogr Sin. 2019;74:1450-1466.

22. Zhou YJ, Zhang CG, Yin SG, Sun T. Coupling coordination and influencing mechanisms of ecological resilience in the Yangtze River Delta region: a resistance-adaptation-recovery framework. Econ Geogr. 2025;45:160-170.

23. Jiang YG, Ouyang JY, Zhang JF. Evolution of social–ecological system resilience and its main obstacle factors in resource-based cities: a case study of Panzhihua. Resour Sci. 2024;46:2064-2077.

24. Yang QQ, Zhang XR, Zhang HQ, Gao YH, Cao XS. The resilience of rural human settlements system and its key factors in traditional agricultural areas of the Loess Plateau: taking Jiaxian county in Northern Shaanxi as an example. J Nat Resour. 2024;39:1101-1118.

25. Yang QQ, Gao YH, Yang XJ. Study on the integration of vulnerability and resilience of rural human settlements system based on grounded theory: evolutionary characteristics, paths and theoretical model. Geogr Res. 2023;42:209-227.

26. Liu YX, Fu BJ, Wang S, Zhao WW, Li Y. Research progress of human-earth system dynamics based on spatial resilience theory. Acta Geogr Sin. 2020;75:891-903.

27. Salvati L, Tombolini I, Perini L, Ferrara A. Landscape changes and environmental quality: the evolution of land vulnerability and potential resilience to degradation in Italy. Reg Environ Change. 2013;13:1223-1233.
28. Luo FH, Liu YX, Peng J, Wu JS. Assessing urban landscape ecological risk through an adaptive cycle framework. Landsc Urban Plan. 2018;180:125-134.
29. Chuang WC, Garmestani A, Eason TN, Spanbauer TL, Fried-Petersen HB, Roberts CP, et al. Enhancing quantitative approaches for assessing community resilience. J Environ Manage. 2018;213:353-362.
30. Hao YQ, Lü YH, Dang H, Lü D, Du C, Wang Y, et al. Optimizing zonal management framework suitable for mountain ecosystems by linking landscape, ecosystem service capacities and bundles nested. J Environ Manage. 2025;389:125998. doi: 10.1016/j.jenvman.2025.125998.
31. Fu BJ, Liu YX, Zhao WW, Wu JG. The emerging "pattern-process-service-sustainability" paradigm in landscape ecology. Landsc Ecol. 2025;40:54. doi: 10.1007/s10980-025-02063-7.
32. Cumming GS. Spatial resilience in social–ecological systems. London: Springer; 2011.
33. Zhang YG. Regional system of man–land relationship evolves into regional system of man-sea relationship: academician Wu Chuanjun's contribution to studies on marine geography. Sci Geogr Sin. 2008;1:6-9.
34. Zeng P, Sheng XL, Cai LW, Xie YQ, Li JX, Wei CP. The conceptual connotation and key issues of the key zone of land–sea integration: based on

1041 the perspective of coastal human settlement environment system research. J
1042 Nat Resour. 2025;40:2920-2934.
1043 35. Zhou LY, Cui WL, Yang F. Spatiotemporal variations and driving forces
1044 analysis of ecosystem water conservation in coastal areas of China. Ecol Indic.
1045 2024;162:112019. doi: 10.1016/j.ecolind.2024.112019.
1046 36. Guo QB, Zhang ZH. Spatial-temporal evolution of factors aggregating ability
1047 in urban agglomeration in the middle reaches of the Yangtze River. Acta
1048 Geogr Sin. 2017;72:1746-1761.
1049 37. Li B, Shi ZY, Han ZL, Tian C. Spatio-temporal difference and influencing
1050 factors of environmental adaptability measurement of human–sea economic
1051 system in Bohai Rim region. Acta Geogr Sin. 2018;73:1121-1132.
1052 38. Han B, Jin XB, Xiang XM, Zhao QL, Lin JH, Hong CQ, et al. Exploration of
1053 ecological restoration pattern and countermeasure along the Yangtze River in
1054 Jiangsu province based on the “element–landscape–system” framework.
1055 J Nat Resour. 2020;35:141-161.
1056 39. Peng J, Lv DN, Dong JQ, Liu YX, Liu QY, Li B. Processes coupling and
1057 spatial integration: characterizing ecological restoration of territorial space in
1058 view of landscape ecology. J Nat Resour. 2020;35:3-13.
1059 40. Fu BJ. The integrated studies of geography: coupling of patterns and process.
1060 Acta Geogr Sin. 2014;69:1052-1059.

41. Zeng QY, Sun CZ. Estimation and influencing factors of carbon storage in terrestrial ecosystems in the Yellow River Basin. Acta Ecol Sin. 2024;44:5476-5493.

42. Gai M, Yue P, Xu JJ, Xu YM. Deconstruction and measurement of coastal resilience based on human-nature system. Geogr Res. 2023;42:2605-2621.

43. Bao YB, Li T, Liu H, Ma T, Wang HX, Liu K, et al. Spatial and temporal changes of water conservation of Loess Plateau in northern Shaanxi province by InVEST model. Geogr Res. 2016;35:664-676.

44. Guo FY, Liu XH, Zhang WB, Xing LY, Wang R, Mamat Z, et al. Evolution of the spatial and temporal patterns of habitat quality and analysis of the driving forces in Yellow River Basin (Henan section) from 2000 to 2040. Geosci. 2024;38:599-611.

45. Wu JS, Cao QW, Shi SQ, Huang XL, Lu ZQ. Spatio-temporal variability of habitat quality in Beijing-Tianjin-Hebei Area based on land use change. Chin J Appl Ecol. 2015;26:3457-3466.

46. Liu Q, Wu ZQ, Feng SY, Li M, Deng L, Fan Y, et al. Identifying the combined impact of human activities and natural factors on China's avian species richness using interpretable machine learning methods. J Environ Manage. 2025;376:124479. doi: 10.1016/j.jenvman.2025.124479.